



Phase-flip transition in volume-mismatched pairs of coupled 1-pentanol drops

Tanushree Roy ^{*}, Sudhanshu Shekhar Chaurasia, and P. Parmananda
Department of Physics, IIT Bombay, Mumbai-400076, Maharashtra, India

 (Received 2 May 2022; accepted 7 September 2022; published 22 September 2022)

We have explored a variety of synchronization domains and observed phase-flip transition in a pair of coupled 1-pentanol drops as a function of the volume mismatch. Both experimental observations and numerical studies are presented. The experiments were carried out in a rectangular channel in a ferroin deionized water solution premixed with some volume of pentanol. A single pentanol drop ($\geq 3 \mu\text{L}$) performs back and forth oscillations along the length of the channel due to the well-known Marangoni forces. In the present work, for a pair of drops, the drop 1 volume was changed from 3 to 5 μL in steps of 1 μL , whereas the drop 2 volume was varied from 1 to 3 μL in steps of 0.5 μL . A systematic investigation of all the possible combinations of the drop volumes showed the presence of three different types of synchrony—*in-phase*, *antiphase*, and *phase-switched*. In-phase synchronization was robust for a volume mismatch of $>3.0 \mu\text{L}$ between the two drops. On the other hand, antiphase synchronization was robust when the volume mismatch was $<2.0 \mu\text{L}$. The *phase-switched* state is a synchronized state involving a phase-flip transition in the time domain. This state was observed for the intermediate range of volume mismatch. Numerically, the system has been investigated using two Stuart-Landau oscillators interacting via a coupling function in the form of Lennard-Jones potential. The numerical results suitably capture both in-phase and antiphase oscillations for a pair of volume-mismatched pentanol drops.

DOI: [10.1103/PhysRevE.106.034614](https://doi.org/10.1103/PhysRevE.106.034614)

I. INTRODUCTION

Self-propelled objects and their mutual interactions provide a platform to study various processes, such as active transport processes in living cells, bacterial locomotion, chemotaxis [1–3], the design of synthetic microswimmers [5] or microrobots [4], and many more [6–9]. A self-propelled object, under certain configurations, is capable of performing oscillatory motion [10–13], rotational motion [14], and stochastic transport [15]. Two or more interacting self-propelled objects in the same environment can give rise to a variety of phenomena, such as pattern formation [16–18], synchronization [19–32], etc. When multiple self-propelled objects are synchronized due to some suitable mode of coupling, their dynamics can lock to a certain phase difference. The self-propelling objects can exhibit either in-phase synchronization (i.e., a phase difference close to zero) or antiphase synchronization (i.e., a phase difference close to π).

Moreover, some research groups have investigated “mode switching” behavior recently. Mode switching implies a transition from one dynamical state to a completely different dynamical state. A mode switching from global oscillations to traveling waves and vice versa has been observed for multiple Belousov-Zhabotinsky (BZ) beads as a function of electric potential by Kuze *et al.* [33]. Another study involves switching from the ballistic to the random mode by changing the chemical state of a droplet [34]. A few other self-propelled

camphor systems also exhibit such mode switching [35,36]. A pentanol droplet on an aqueous surface has been studied by Nagai *et al.* [37,38]. It was observed that the dynamics of the droplet switched from irregular translational motion to vectorial motion when the droplet volume was changed from 0.1 to 0.1–200 μL .

The self-propulsion mechanism of a pentanol drop on an aqueous medium is derived from the instantaneous surface tension imbalance around the drop. The imbalance in the surface tension profile is followed by a spontaneous symmetry breaking in the concentration gradient around the drop due to the well-known Marangoni effect [8]. In the case of multiple self-propelled drops, their coupled behavior is derived from the mutual interplay of their surface tension gradients.

Similar to the mode-switching behavior observed previously in self-propelled systems (as mentioned), here we report the “phase-flip” transition [39,40] as a function of a system parameter (i.e., volume mismatch). In this case, the relative phase difference between the oscillatory dynamics of two synchronized 1-pentanol drops switches from 0 to π as the volume mismatch is varied. However, for certain volume mismatches, it can happen that the synchronized oscillations can abruptly switch from in-phase to antiphase as time progresses. This behavior is termed “phase-switched” dynamics. To reiterate, the “phase-switched” dynamics emerge by virtue of the underlying phase-flip transition.

Experimental observations were verified numerically considering two bidirectionally coupled Stuart-Landau [41] oscillators. The coupling function was chosen to be the Lennard-Jones [42] potential. The numerical results are able to qualitatively capture the in-phase and antiphase synchronization. The volume mismatch between the drops is

^{*}Present address: Centro de Investigación en Ciencias (IICBA), UAEM, Avenida Universidad 1001, Colonia Chamilpa, CP 62209 Cuernavaca, Morelos, Mexico.

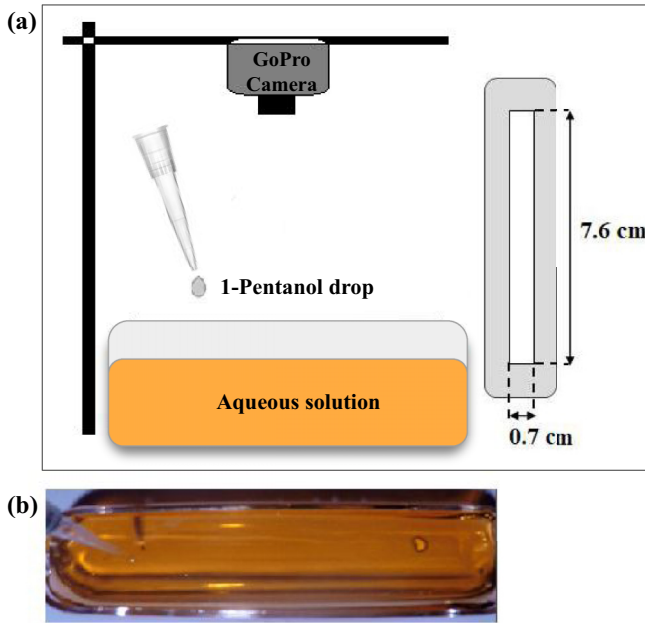


FIG. 1. (a) Left: Schematic of the experimental setup: a rectangular quartz boat [outer dimensions: 10.0 cm (L), 2.5 cm (W), 1.7 cm (H); inner dimensions: 9.7 cm (L), 2.3 cm (W), 1.5 cm (H)] containing an aqueous solution including ferroin and 1-pentanol. Right: The linear channel [outer dimensions 9.6 cm (L) \times 2.1 cm (W) and inner dimensions 7.6 cm (L) \times 0.7 cm (W)] with a thickness of 90 μm . (B) Top view of the rectangular boat in the experiments shows that the smaller 1-pentanol drop is introduced in the solution when the bigger drop is already present.

analogous to the mismatch between a pair of coefficients for the coupling function in the simulations.

This paper is organized into six different sections following the Introduction in Sec. I. The experimental setup and related protocols are discussed in Sec. II. In Sec. III, all the experimental observations are presented. The numerical model is discussed in Sec. IV, followed by the numerical results presented in Sec. V. Finally, in Sec. VI, a brief discussion of the results is provided.

II. EXPERIMENTS

Figure 1(a) presents a schematic diagram of the experimental setup (left) and the rectangular channel (right). Figure 1(b) shows the top view of the quartz boat employed for the experiments. The experiments were performed with a pair of 1-pentanol drops moving in a rectangular channel. The aqueous solution was prepared from 15 mL of deionized (DI) water adding 70 μL of ferroin and 350 μL of 1-pentanol. Ferroin was used as a dye. A thin transparent plastic sheet (of thickness 90 μm , used in lamination) with a channel of inner dimensions of 0.7 cm in width and 7.6 cm in length was placed to float on the aqueous phase [shown in Fig. 1(a)]. The temperature was maintained between 300 ± 2.5 K, and all the experiments were performed in an open environment but without allowing any cross-ventilation across the room. The maximum drop volume used was 5 μL and the minimum was 1 μL . In our study, the bigger drop (i.e., drop 1) volume

Volume	Drop1		
	5 μL	4 μL	3 μL
Drop 2			
1.0 μL	A. In-phase	A. In-phase B. Phase-switched	A. In-phase B. Anti-Phase C. Phase-switched (Rare)
1.5 μL	A. In-phase	A. Phase-switched B. Anti-phase	A. Anti-phase
2.0 μL	A. Phase-switched B. Anti-Phase (Rare)	A. Phase-switched B. Anti-phase	A. Anti-phase
2.5 μL	A. Phase-switched B. Anti-phase	A. Anti-phase	A. Anti-phase
3.0 μL	A. Anti-phase B. Phase-switched (Rare)	A. Anti-phase	A. Anti-phase

FIG. 2. Overview of the different coupled dynamics observed for all the volume-mismatched pairs of 1-pentanol drops.

varied from 3 to 5 μL in steps of 1 μL , and the smaller drop (i.e., drop 2) volume was varied from 1 to 3 μL in steps of 0.5 μL . For all the experiments, the bigger drop was introduced at first in the air-aqueous interface, and within 5–10 s the smaller drop goes in the channel, as shown in Fig. 1(b) (the smaller drop is being introduced when the bigger drop is already present). The reason for following this protocol was to minimize the chances of smaller drops breaking or sticking to the edges of the channel. When the drop volume is lower than 3 μL , in addition to the back and forth motion, it also performs a little zigzag motion along the channel, and this zigzag motion increases as the drop volume is further lowered. This zigzag motion sometimes causes the drop to stick to the edges and thus the drop loses some volume at the edge. Due to this loss of volume, the drop experiences a high surface-tension gradient from the edge to the waterway. So, it quickly tries to return from the edge to the main waterway, i.e., from the low surface-tension region to the high surface-tension region. During this sudden movement, (i) either the drop can quickly attach to the opposite edge of the channel and can lose some further volume of pentanol there, or (ii) the deformation in the drop can cause it to break into droplets. To avoid this, the bigger pentanol drop was placed first in the solution. This way, the movement of the bigger drop in the channel lowers the chances for the smaller drop to get attached to any of the edges of the channel.

All the videos were captured using a GoPro camera with a frame rate of 30 frames per second. The time-series analysis was performed using OpenCV and MATLAB.

III. EXPERIMENTAL RESULTS

A global summary of the coupled dynamics observed experimentally in all the pairs of 1-pentanol drops is presented in the table shown in Fig. 2. It can be observed that in some pairs there exist multiple stable states with varying degrees of robustness. For example, pair (3,1) shows in-phase, antiphase, and phase-switched modes of synchrony among which only in-phase and antiphase states are robust, whereas the appearance of phase-switched dynamics is less frequent. Similarly, for pair (5,2), phase-switched is the dominant state,

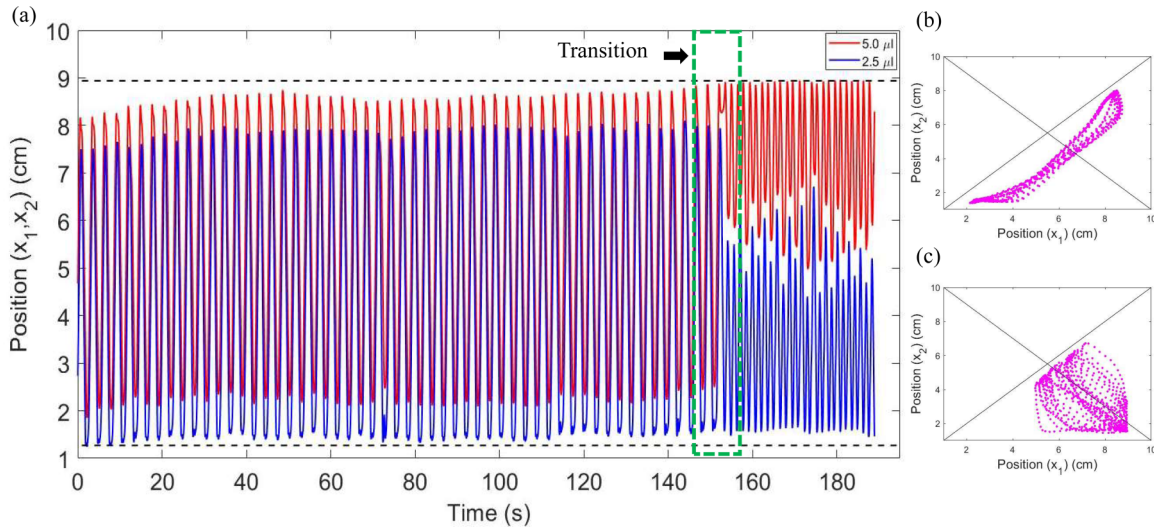


FIG. 3. (a) A complete time series showing phase-switched oscillations for the pair (5,2.5), where x_1 (cm) vs time (s) corresponds to the oscillations of $5 \mu\text{L}$ and x_2 (cm) vs time (s) for $2.5 \mu\text{L}$. Dotted black lines represent channel edges. The rectangular green box in the dashed line indicates the region of transition from in-phase to antiphase oscillatory modes. The video file is attached in the Supplemental Material [43] as Movie 2. (b) Phase portraits x_2 (cm) vs x_1 (cm) correspond to the dynamics within 20–50 s. (c) Phase portraits x_2 (cm) vs x_1 (cm) correspond to the dynamics within 159–189 s.

and antiphase is less frequent. However, for pair (5,2.5), both phase-switched and antiphase are almost equally probable.

In total, we have studied the dynamics of 15 sets of pairs, among which pair (3,3) has already been reported in our previous work [30]. The dynamics related to each pair have been studied multiple times to verify the robustness of our observations. However, the number of experiments performed was not enough to provide a quantitative measure or a statistically significant analysis. The main goal was more to survey different domains of observed coupled dynamics.

At first, the dynamics are discussed for the total volume of $8 \mu\text{L}$. In this case, the volume of drop 1 is $5 \mu\text{L}$, and the drop 2 volume is $3 \mu\text{L}$. For the sake of convenience, let us denote the pair of 5 and $3 \mu\text{L}$ drops as pair (5,3), and the same notation will be followed throughout for other combinations as well. Every time, for a fixed volume of drop 1, the drop 2 volume was lowered systematically to observe the different domains of coupled dynamics.

In all the experimental position time-series plots, the drop 1 (i.e., higher volume) time series has been plotted in “red” and the drop 2 (i.e., lower volume) time series is presented in “blue.” In each case, any “stable dynamics” or a “stable state” implies that the oscillations will last for at least 10 cycles.

Pair (5,3): In this case, both the volume mismatch and the individual drop sizes allow them to perform mostly antiphase oscillations. A complete time series is shown in Fig. S1 in the Supplemental Material [43]. The corresponding short video file is attached in the Supplemental Material [43] as Movie 1. For this pair, the phase-switched dynamics appeared only once out of seven successful experimental runs.

Pair (5,2.5): This pair of drops exhibit both phase-switched and antiphase modes of synchronization. Here, the time series are presented only for the mixed-phase dynamics. Figure 3(a) presents the full time series showing the transition region. Figure 3(b) shows the phase portraits within a time window of 20–50 s confirming in-phase synchrony, and Fig. 3(c)

confirms the antiphase synchrony within a time window of 159–189 s. The corresponding short video file is attached in the Supplemental Material [43] as Movie 2. In Fig. 3(a), it can be observed that the frequency of the antiphase oscillations is higher than the frequency of in-phase oscillations. This observation is consistent with the previous study [39] on phase-flip transition. A full time series related to purely antiphase oscillations is presented in Fig. S2 in the Supplemental Material [43].

Pair (5,2): In this case, the drops exhibit long in-phase oscillations followed by short antiphase oscillations, i.e., phase-switched dynamics. Figure S3 shows the full position time series of the drops in the Supplemental Material [43]. The corresponding short video file is attached in the Supplemental Material [43] as Movie 3.

Pair (5,1.5): This pair performs in-phase oscillations presented in Fig. S4 in the Supplemental Material [43]. Interestingly, in this pair, the drops have also been observed to cross each other and switch sides in the channel area. The corresponding short video file is attached in the Supplemental Material [43] as Movie 4.

Pair (5,1): This pair shows in-phase oscillations as shown in Fig. 4. In this case, drop 2 (i.e., $1 \mu\text{L}$) is trapped in the flow field governed by the movement of drop 1 (i.e., $5 \mu\text{L}$). The corresponding short video file is attached in the Supplemental Material [43] as Movie 5.

Pairs (4,3) and (4,2.5): Both pairs synchronize via antiphase oscillations, and their full time series are presented in Figs. S5 and S6, respectively, in the Supplemental Material [43]. The corresponding video files are attached as Movie 6 for pair (4,3) and Movie 7 for pair (4,2.5).

Pair (4,2): This pair shows both phase-switched and antiphase mode of synchrony, but the phase-switched state is more robust than the antiphase. Out of six experimental runs, the phase-switched dynamics was observed four times and the antiphase dynamics was observed only two times. Figure 5(a)

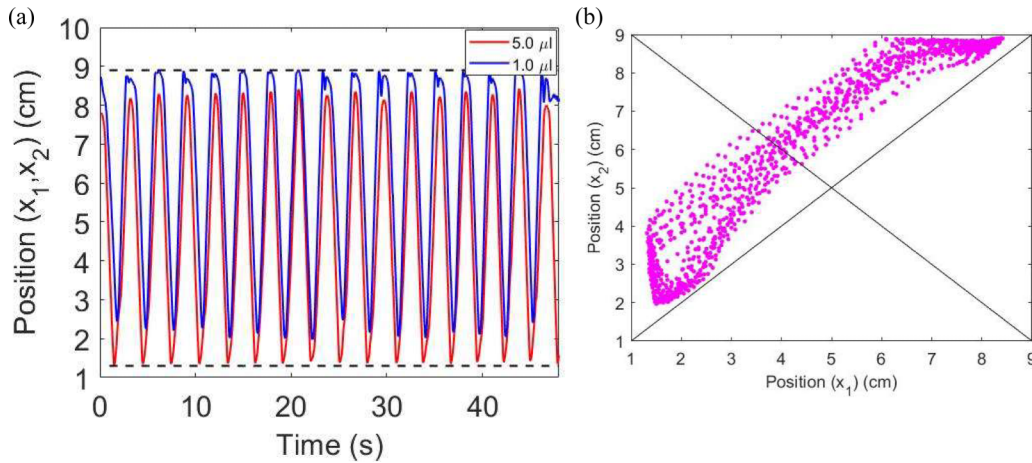


FIG. 4. (a) A complete time series showing in-phase oscillations for the pair (5,1), where x_1 (cm) vs time (s) corresponds to the oscillations of $5 \mu\text{L}$ and x_2 (cm) vs time (s) for $1 \mu\text{L}$. Dotted black lines represent channel edges. The video file is attached in the Supplemental Material [43] as Movie 5. (b) Phase portraits correspond to x_2 (cm) vs x_1 (cm).

shows the full time series showing a transition from an in-phase to an antiphase mode of synchrony. Figure 5(b) shows the phase portraits for the dynamics in a range of 20–50 s, and Fig. 5(c) presents the phase portraits that correspond to the dynamics within 70–100 s. Here also, in Fig. 5(a), we can observe that the frequency of the out-of-phase dynamics is higher than that of the in-phase dynamics. Also, the amplitudes of the in-phase oscillations are almost double the amplitudes for the antiphase oscillations. This is because, during in-phase oscillations, the drops have the whole channel length available for their synchronized sailing, but during antiphase oscillations, the repulsive interaction between the drops allows each of them to occupy only half of the channel length. The corresponding short video file is attached in the Supplemental Material [43] as Movie 8.

Pair (4,1.5): This pair is mostly unstable. The drops quickly merge with each other. However, a few times when the coalescence could be avoided, the drops mostly exhibited either phase-switched or antiphase mode of oscillations. Both these dynamics are presented in Fig. S7 in the Supplemental Material [43]. Due to the highly unstable nature of this pair, the time series are short. The corresponding short video files are attached in the Supplemental Material [43] as Movies 9a and 9b.

Pair (4,1): This pair is also highly unstable as the drops mostly merge with each other. A few times, when the merging could be avoided, the pair showed both in-phase and phase-switched modes of synchronization. But, the phase-switched dynamics is the most robust one. In that case, the drops mostly start with in-phase oscillations, and after some time they go on

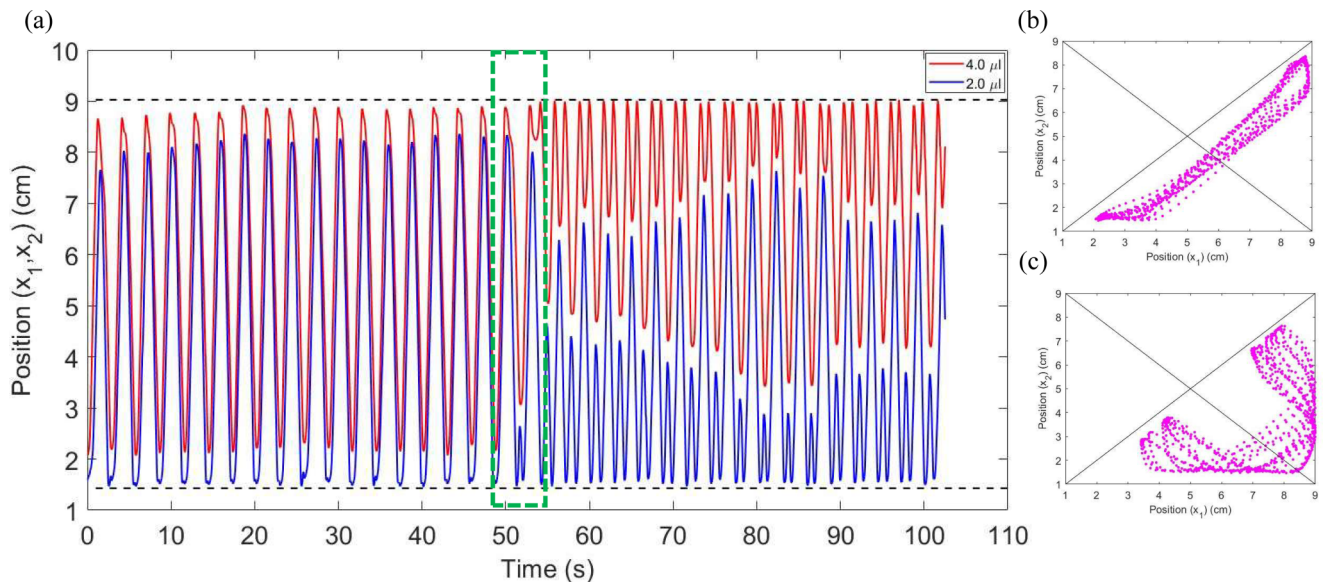


FIG. 5. (a) A complete time series showing phase-switched dynamics for the pair (4,2), where x_1 (cm) vs time (s) corresponds to the oscillations of $4 \mu\text{L}$ and x_2 (cm) vs time (s) for $2 \mu\text{L}$. Dotted black lines represent channel edges. The rectangular green box in the dashed line indicates the region of transition from in-phase to antiphase oscillatory modes. The video file is attached in the Supplemental Material [43] as Movie 8. (b) Phase portraits corresponding to the dynamics within 20–50 s. (c) Phase portraits corresponding to the dynamics within 70–100 s.

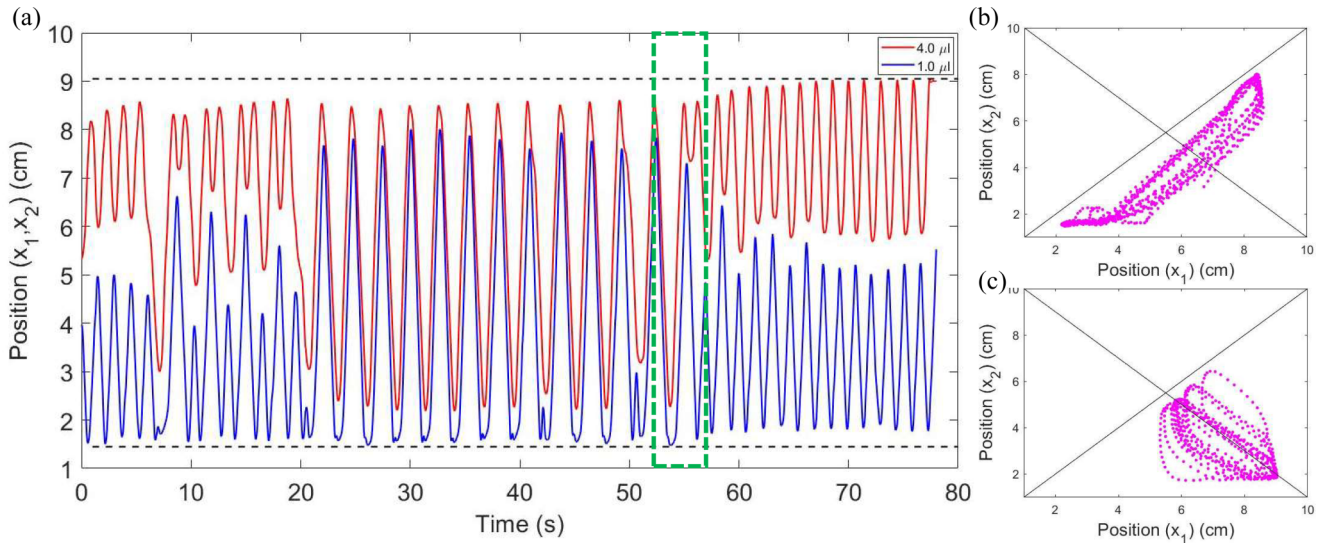


FIG. 6. Phase-switched dynamics in a pair of 4.0 and 1.0 μL drops. (a) The oscillations time series show the transition from in-phase to out-of-phase dynamics. The video file is attached in the Supplemental Material [43] as Movie 10. Parts (b) and (c) present the phase portraits corresponding to in-phase and antiphase domains.

performing antiphase oscillations. Out of five successful experimental runs, the phase-switched dynamics were observed three times. Figure 6(a) shows the position time series of the drops, and Figs. 6(b) and 6(c) are the phase portraits confirming the in-phase and antiphase oscillations, respectively. The corresponding short video file is attached in the Supplemental Material [43] as Movie 10.

Pairs (3,3), (3,2.5), and (3,2): All these pairs show antiphase oscillations. Antiphase mode of synchronization was already reported for pair (3,3) in our previous work. The time series and the phase portraits corresponding to pairs (3,2.5) and (3,2) are presented in the Supplemental Material [43] in Figs. S8 and S9, respectively. The corresponding short video files are attached in the Supplemental Material [43] as Movies 11 and 12, respectively.

Pair (3,1.5): This pair also performs antiphase oscillations. The time series and corresponding phase portrait are shown

in Figs. 7(a) and 7(b), respectively. The corresponding short video file is attached in the Supplemental Material [43] as Movie 13.

Pair (3,1): This pair is extremely unstable. In this case, the pair can synchronize via both in-phase or antiphase oscillations. The dynamics mostly follow in-phase transient oscillations but can settle into performing either in-phase [Fig. 8(a)] or antiphase [Fig. 8(c)]. Figures 8(b) and 8(d) are the phase portraits of the dynamics corresponding to Figs. 8(a) and 8(c), respectively. The corresponding short video files are attached in the Supplemental Material [43] as Movies 14a and 14b. The phase-switched dynamics are rare.

IV. NUMERICAL MODEL

The period-1 oscillations of a single pentanol drop are modeled by using the equations of an uncoupled

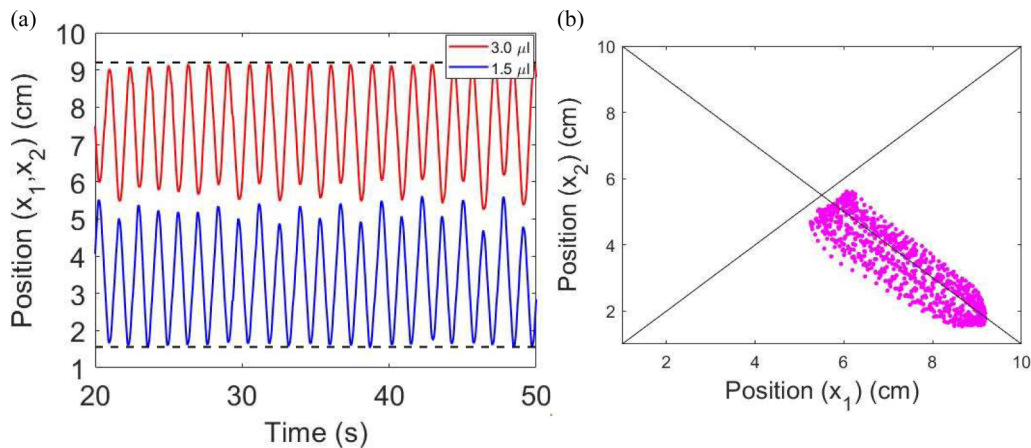


FIG. 7. (a) A partial time series showing antiphase oscillations in a pair of 3.0 and 1.5 μL drops. The dotted black lines indicate the edges of the rectangular channel. Extended time series are presented in Fig. S10 in the Supplemental Material [43]. The video file is attached in the Supplemental Material [43] as Movie 13. (b) Phase portraits show how x_2 (cm) is changing with respect to x_1 (cm).

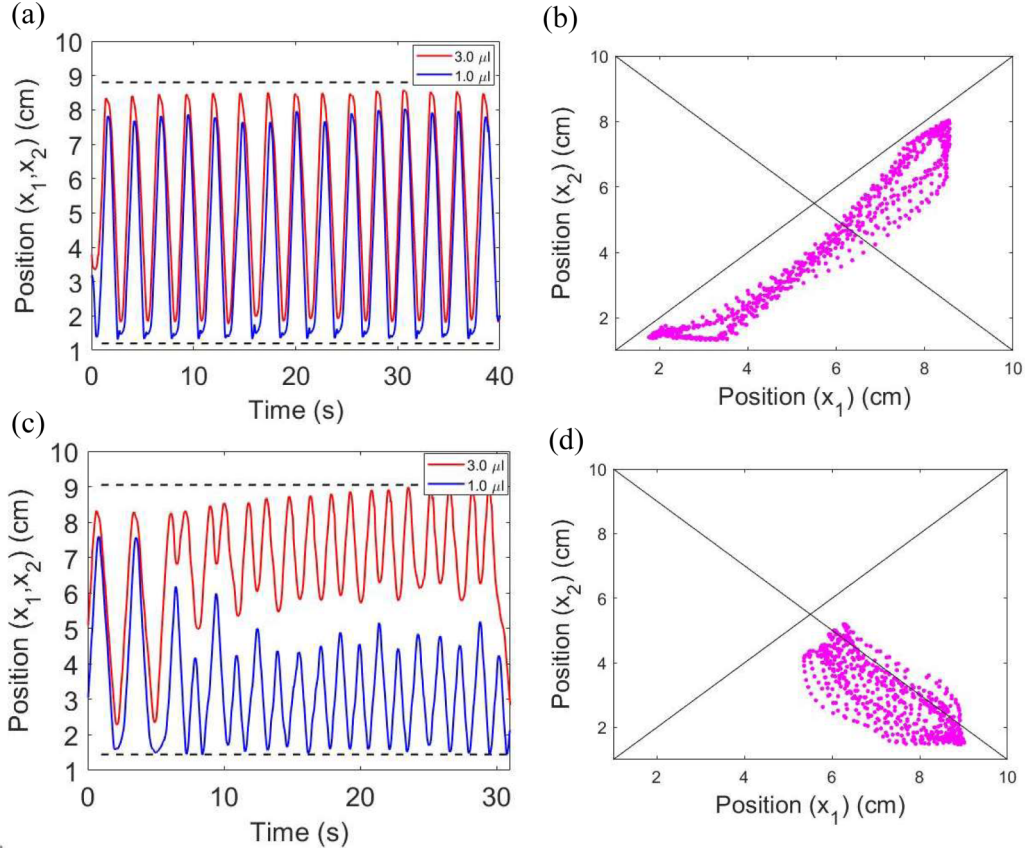


FIG. 8. The two most possible dynamics observed for a pair of 3.0 and 1.0 μL drops. Part (a) shows in-phase oscillations of the drops, and the corresponding phase portraits are shown in (b). The video file is attached in the Supplemental Material [43] as Movie 14a. Part (c) shows the antiphase oscillations of the drops, and the corresponding phase portraits are shown in (d). The dotted black lines both in (a) and (c) indicate the edges of the rectangular channel. The corresponding video file is attached in the Supplemental Material [43] as Movie 14b.

Stuart-Landau (SL) oscillator as given by Eq. (1). The set of equations governing the motion of a single oscillator is as follows:

$$\begin{aligned}\dot{x}(t) &= x(t)\{1 - [x(t)^2 + y(t)^2]\} - \omega y(t), \\ \dot{y}(t) &= y(t)\{1 - [x(t)^2 + y(t)^2]\} + \omega x(t).\end{aligned}\quad (1)$$

In the equations, variables $x(t)$ and $y(t)$, respectively, denote the *position* and the *velocity* of the moving oscillator, whereas ω represents the *natural frequency* of the oscillator.

To capture the qualitative features of the experimental observations for a pair of volume-mismatched pentanol drops, we have considered two Stuart-Landau oscillators. The oscillators are bidirectionally coupled with a slight mismatch in their autonomous frequencies in an effort to mimic the experiments. The sets of equations governing the motion of two coupled Stuart-Landau oscillators are given by the following equations:

$$\begin{aligned}\dot{x}_1(t) &= x_1(t)\{1 - [x_1(t)^2 + y_1(t)^2]\} - \omega_1 y_1(t), \\ \dot{y}_1(t) &= y_1(t)\{1 - [x_1(t)^2 + y_1(t)^2]\} + \omega_1 x_1(t) \\ &\quad - \beta_1 * V(r), \\ \dot{x}_2(t) &= x_2(t)\{1 - [x_2(t)^2 + y_2(t)^2]\} - \omega_2 y_2(t), \\ \dot{y}_2(t) &= y_2(t)\{1 - [x_2(t)^2 + y_2(t)^2]\} + \omega_2 x_2(t) \\ &\quad + \beta_2 * V(r).\end{aligned}\quad (2)$$

β_1 and β_2 are the coefficients of the coupling function, which is $V(r)$. The coupling function has been chosen as the form of Lennard-Jones potential as given in Eq. (3). $r(t)$ is the time-dependent separation between the oscillators, and is defined as $|x_1 - x_2|$,

$$V(r) = V_0 + \varepsilon \left[\left(\frac{a}{r(t)} \right)^{12} - \left(\frac{a}{r(t)} \right)^6 \right]. \quad (3)$$

In our simulations, the parameters are $V_0 = 0.1$, $\varepsilon = 1$, $a = 0.38$, $\omega_1 = 5.05$, and $\omega_2 = 5.00$. The initial set of conditions were chosen as $(x_1, y_1)|_{(t=0)} = (0.9, -0.1)$ and $(x_2, y_2)|_{(t=0)} = (-1.0, -1.0)$. The set of equations were solved using the Runge-Kutta fourth-order (RK4) method. The time step was chosen as $dt = 0.01$. The volume-mismatched drops in experiments are analogous to the pair of SL oscillators with $\beta_1 \neq \beta_2$.

V. NUMERICAL RESULTS

The mismatch in the values of β_1 and β_2 is similar to the mismatch in the volumes of drops in experiments. For the sake of simplicity, the β_1 value was fixed and the β_2 value was varied to observe in-phase and antiphase oscillations. All the results are presented after discarding the transients (i.e., the first 500 time units) from the time series.

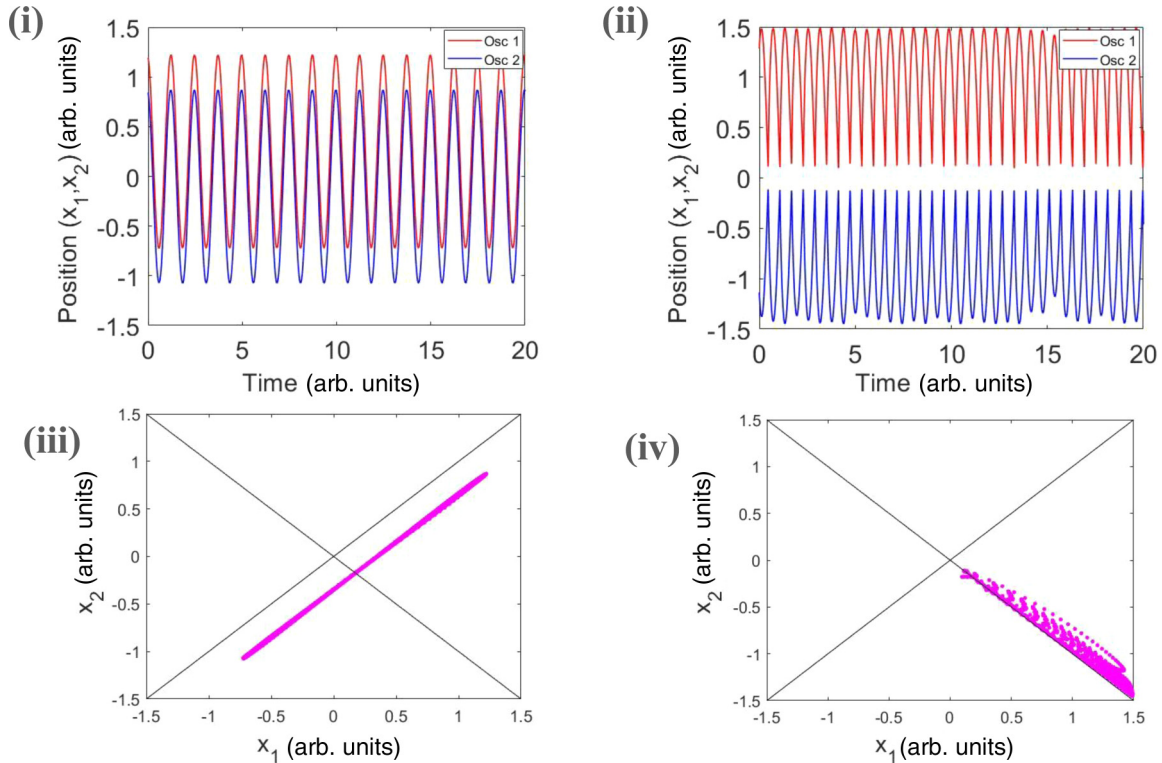


FIG. 9. (i) Time series are showing the in-phase oscillations for $\beta_1 = 1.0$ and $\beta_2 = 0.4$, and the corresponding phase portraits are shown in (ii). (iii) Time series are showing the antiphase oscillations for $\beta_1 = 1.0$ and $\beta_2 = 0.62$, and the corresponding phase portraits are shown in Fig. (iv).

(i) In-phase oscillations were obtained for $\beta_1 = 1.0$ and $\beta_2 = 0.40$. The corresponding time series and the phase-space plots are shown in Figs. 9(i) and 9(iii), respectively.

(ii) Antiphase oscillations were obtained for $\beta_1 = 1.0$ and $\beta_2 = 0.62$. The corresponding time series and the phase-space plots are shown in Figs. 9(ii) and 9(iv), respectively.

The numerics are able to capture both in-phase and antiphase dynamics observed in the experiments and thus confirms the phase-flip transition by suitable tuning of the mismatch between β_1 and β_2 values. However, it is unable to capture the phase-switched state observed experimentally.

VI. DISCUSSION AND CONCLUSIONS

Based on the volume mismatch between the pair of drops, mainly three different types of coupled dynamics were observed. These are (i) in-phase, (ii) phase-switched, and (iii) antiphase dynamics. When the volume mismatch is $> 3.0 \mu\text{L}$, the drops always synchronize via stable in-phase oscillations. In that case, the pair is analogous to the master-slave configuration where the bigger drop acts as a master and controls the movement of the smaller (i.e., slave) drop. The smaller drop is trapped in the flow-field created by the bigger drop and thus moves in tandem with the bigger drop exhibiting in-phase synchronization. This in-phase synchronization was observed for pair (6,1) as well (not presented here). For a volume mismatch of $\geq 2.0 \mu\text{L}$ and $\leq 3.0 \mu\text{L}$, the pairs show multiple stable states including the phase-switched dynamics. At a lower level of volume mismatch in the range of $< 2.0 \mu\text{L}$, the drops always synchronize via antiphase oscillations. In

this case, the volume mismatch is not sufficient to let the bigger drop control the movement of the smaller drop.

In the “phase-switched” state, drops first synchronize via stable in-phase oscillations, and after some time they make a transition from stable in-phase to perform stable antiphase oscillations. A possible explanation for the appearance of this “phase-switched” state is the following. Being in the in-phase mode of synchrony for a long time, the concentration gradients around the drops are modified in such a way that the bigger drop can no longer trap the movement of the smaller drop. Therefore, in the end, the drops start moving in antiphase. However, it needs to be pointed out that the “phase-switched” dynamics imply phase-flip transition as a function of time. The drops show a transition from stable in-phase to stable antiphase oscillations as time progresses. The reverse (i.e., transition from stable antiphase to stable in-phase) was not observed experimentally. Moreover, it was observed that the frequency of the antiphase oscillations is always higher than the in-phase oscillations. On the contrary, the amplitudes of the antiphase oscillations are always lower than the amplitudes of the in-phase oscillations. A pair of drops readjusts their speeds according to their dynamical state. Therefore, a pair of drops move with faster speed while performing antiphase oscillations than in-phase oscillations.

Another set of experimental observations shows that the total duration of the stable state is highly dependent upon both volume mismatch and on the individual drop sizes. When the smaller drop volume is $\leq 1.5 \mu\text{L}$ and the volume mismatch between the drops is approximately in the range of $2\text{--}2.5 \mu\text{L}$,

the coupled dynamics persists for a shorter period of time. For example, the stable state for pair (4,2) exists for a longer period of time than the dynamics observed for pair (3,1), though the volume mismatch is exactly the same (i.e., $2 \mu\text{L}$) for both. Similarly, the duration of the stable state observed for the pair (4,1.5) is short. In such cases, the drops mostly merge with each other. Moreover, in the current channel configuration, it has been observed that a pair of drops exhibit stable dynamics (i.e., one or multiple stable states) only when one of the drops is of $3 \mu\text{L}$ volume. This is why the coupled dynamics for the pair of ($1 \mu\text{L}$, $1 \mu\text{L}$) and a pair ($2 \mu\text{L}$, $2 \mu\text{L}$) are not reported in the present work.

Figure 2 summarizes all the domains of synchronization observed for individual pairs of 1-pentanol drops. At a particular drop 1 volume, the mode of synchrony switches from in-phase to antiphase as the volume mismatch is lowered. For example, pair (5,1) shows in-phase synchrony, but pair (5,3) shows antiphase synchrony. Such a phase-flip transition has been confirmed multiple times for other pairs as well. Therefore, it is evident that the phase-flip transition can be achieved by tuning the volume mismatch between the drops. The level of volume mismatch from low to high switches the mode of coupling from “bidirectional” to “unidirectional.” In the bidirectional mode of coupling, the drops interact repulsively, and in the unidirectional coupling mode, the drops are attractive to each other. Hence, the switching of the coupling mode is the underlying reason for the occurrence of the phase-flip transition.

The numerics capture the phase-flip transition from in-phase to antiphase oscillations as a function of parameter mismatch and thus support the experimental observations. The difference in the values of β_1 and β_2 decides the coupled state of the system. When the difference between these coefficients is high, the oscillators show in-phase synchrony, and for small difference the oscillators perform antiphase synchronization. However, the phase-switched state was absent in the numerics.

The present work explains that suitable tuning of the volume mismatch results in altering the underlying mode of coupled dynamics. Our results provide some groundwork in the field of self-propelled objects and active matter. This can help to develop and design artificial motors or microswimmers to study chemotactic movements. Furthermore, our observations can be useful to study drug delivery in the intracellular transport processes. As per the requirement, only some amount of volume/size mismatch between two self-propelled objects can decide their mode of interactions, which can further aid in performing any specific tasks.

ACKNOWLEDGMENTS

We acknowledge the financial support from DST, Government of India with Project No. 16DST045 (DST SERB Grant no.-EMR/2016/000275).

- [1] J. Čejková, M. Novak, F. Stepanek, and M. M. Hanczyc, *Langmuir* **30**, 11937 (2014).
- [2] S. Lach, S. M. Yoon, and B. A. Grzybowski, *Chem. Soc. Rev.* **45**, 4766 (2016).
- [3] B. Liebchen and H. Löwen, *Acc. Chem. Res.* **51**, 2982 (2018).
- [4] K. Yoshida and H. Onoe, *Adv. Intell. Syst.* **4**, 2100248 (2022).
- [5] E. R. Kay, D. A. Leigh, and F. Zerbetto, *Angew. Chem. Int. Ed.* **46**, 72 (2007).
- [6] S. Sengupta, M. E. Ibele, and A. Sen, *Angew. Chem. Int. Ed.* **51**, 8434 (2012).
- [7] N. J. Suematsu and S. Nakata, *Chem. Eur. J.* **24**, 6308 (2018).
- [8] *Self-Organized Motion: Physicochemical Design Based on Non-linear Dynamics*, edited by S. Nakata, V. Pimienta, I. Lagzi, H. Kitahata, and N. J. Suematsu (Royal Society of Chemistry, 2018).
- [9] R. Kapral, *J. Chem. Phys.* **138**, 020901 (2013).
- [10] Y. Koyano, T. Sakurai, and H. Kitahata, *Phys. Rev. E* **94**, 042215 (2016).
- [11] Y. Xu, N. Takayama, H. Er, and S. Nakata, *J. Phys. Chem. B* **125**, 1674 (2021).
- [12] M. Nagayama, S. Nakata, Y. Doi, and Y. Hayashima, *Physica D* **194**, 151 (2004).
- [13] J. Sharma, I. Tiwari, P. Parmananda, and M. Rivera, *Phys. Rev. E* **105**, 014216 (2022).
- [14] V. Pimienta, M. Brost, N. Kovalchuk, S. Bresch, and O. Steinbock, *Angew. Chem. Int. Ed.* **50**, 10728 (2011).
- [15] A. Biswas, J. M. Cruz, P. Parmananda, and D. Das, *Soft Matter* **16**, 6138 (2020).
- [16] H. Kitahata, N. Yoshinaga, K. H. Nagai, and Y. Sumino, *Dynamics of droplets, Pattern Formations and Oscillatory Phenomena* (Elsevier, Amsterdam, 2013), pp. 85–118.
- [17] D. Levis and B. Liebchen, *Phys. Rev. E* **100**, 012406 (2019).
- [18] B. Zhang, A. Sokolov, and A. Snezhko, *Nat. Commun.* **11**, 1 (2020).
- [19] S. Nakata, Y. Doi, and H. Kitahata, *J. Phys. Chem. B* **109**, 1798 (2005).
- [20] T. Song, H. Kim, S. W. Son, and J. Jo, *Phys. Rev. E* **101**, 022613 (2020).
- [21] K. Ito, T. Ezaki, S. Suzuki, R. Kobayashi, Y. Hara, and S. Nakata, *J. Phys. Chem. B* **120**, 2977 (2016).
- [22] Y. J. Chen, K. Sadakane, H. Sakuta, C. Yao, and K. Yoshikawa, *Langmuir* **33**, 12362 (2017).
- [23] S. Nakata, K. Kayahara, M. Kuze, E. Ginder, M. Nagayama, and H. Nishimori, *Soft Matter* **14**, 3791 (2018).
- [24] A. Aubret, M. Youssef, S. Sacanna, and J. Palacci, *Nat. Phys.* **14**, 1114 (2018).
- [25] J. Sharma, I. Tiwari, D. Das, P. Parmananda, V. S. Akella, and V. Pimienta, *Phys. Rev. E* **99**, 012204 (2019).
- [26] D. Levis, I. Pagonabarraga, and B. Liebchen, *Phys. Rev. Res.* **1**, 023026 (2019).
- [27] S. Sato, H. Sakuta, K. Sadakane, and K. Yoshikawa, *ACS Omega* **4**, 12766 (2019).
- [28] M. A. Budroni, K. Torbensen, S. Ristori, A. Abou-Hassan, and F. Rossi, *J. Phys. Chem. Lett.* **11**, 2014 (2020).
- [29] C. H. Meredith, P. G. Moerman, J. Groenewold, Y. J. Chiu, W. K. Kegel, A. van Blaaderen, and L. D. Zarzar, *Nat. Chem.* **12**, 1136 (2020).

- [30] T. Roy, S. S. Chaurasia, J. M. Cruz, V. Pimienta, and P. Parmananda, *Soft Matter* **18**, 1688 (2022).
- [31] D. K. Verma, H. Singh, A. Q. Contractor, and P. Parmananda, *J. Phys. Chem. A* **118**, 4647 (2014).
- [32] D. K. Verma, H. Singh, P. Parmananda, A. Q. Contractor, and M. Rivera, *Chaos* **25**, 064609 (2015).
- [33] M. Kuze, M. Horisaka, N. J. Suematsu, T. Amemiya, O. Steinbock, and S. Nakata, *J. Phys. Chem. B* **125**, 3638 (2021).
- [34] N. J. Suematsu, Y. Mori, T. Amemiya, and S. Nakata, *J. Phys. Chem. Lett.* **12**, 7526 (2021).
- [35] I. Tiwari, P. Parmananda, and R. Chelakkot, *Soft Matter* **16**, 10334 (2020).
- [36] K. Nishi, K. Wakai, T. Ueda, M. Yoshii, Y. S. Ikura, H. Nishimori, S. Nakata, and M. Nagayama, *Phys. Rev. E* **92**, 022910 (2015).
- [37] K. Nagai, Y. Sumino, H. Kitahata, and K. Yoshikawa, *Phys. Rev. E* **71**, 065301(R) (2005).
- [38] K. Nagai, Y. Sumino, and K. Yoshikawa, *Colloids Surf., B* **56**, 197 (2007).
- [39] J. M. Cruz, J. Escalona, P. Parmananda, R. Karnatak, A. Prasad, and R. Ramaswamy, *Phys. Rev. E* **81**, 046213 (2010).
- [40] A. Sharma, M. Dev Shrimali, and S. Kumar Dana, *Chaos* **22**, 023147 (2012).
- [41] Y. Kuramoto, Reductive perturbation method, in *Chemical Oscillations, Waves, and Turbulence*, Springer Series in Synergetics Vol. 19 (Springer, Berlin, 1984).
- [42] J. A. Lemkul, Pairwise-additive and polarizable atomistic force fields for molecular dynamics simulations of proteins, *Prog. Mol. Biol. Transl. Sci.* **170**, 1 (2020).
- [43] See Supplemental Material at <http://link.aps.org/supplemental/10.1103/PhysRevE.106.034614> for all the time series corresponding to the volume-mismatched pairs, including all the video files.